Doctoral Dissertation

A Survey on Image Denoise

Department of Artificial Intelligence Convergence

Graduate School, Chonnam National University

NGUYEN, Van-Tai

August 2021

A Survey on Image Denoise

Department of Artificial Intelligence Convergence

Graduate School, Chonnam National University

NGUYEN, Van-Tai

Supervised by Professor KIM, Yong-B

A dissertation submitted in partial fulfillment of the requirements for the Doctor of Engineering in Artificial Intelligence Convergence.

Committee in Charge:

KIM, Yong-B _____

KIM, Yong-B _____

KIM, Yong-B _____

KIM, Yong-B _____

KIM, Yong-B _____

August 2021

Table of Contents

List of Figures

List of Tables

A Survey on Image Denoise

NGUYEN, Van-Tai

Department of Artificial Intelligence Convergence
Graduate School, Chonnam National University
(Supervised by Professor KIM, Yong-B)

(Abstract)

Denoising is a pre-processing step in the digital image processing system. It is also a typical image processing challenge. Many works proposed to solve problems with new approaches. They can be divided into two main categories: spatial-based or transform-based. Some denoising methods apply in both spatial and transform domains.

The goal of this paper focuses on reviewing denoise methods, classifying them into different categories, and identifying new trends. Moreover, we do experiments to compare the pros, cons of methods in surveys.

1. INTRODUCTION

Digital image can degraded by noise in the process of capture, acquisition, processing and transmission. Therefore, image denoising is one of the fundamental challenges in the field of image processing and computer vision with the objective to eliminate the noise from given noisy image in data acquisition to predict original image. A good image denoising model is eliminating noise as much as possible while preserving the characteristics of the image such as edges, corners and other sharp structures, etc.[1]

Two main approach to image denoising is based on spatial domain, and transform domain. Besides, there are some image denoising methods implemented in both spatial and transform domain.

Approaching denoise in spatial domain, Tomasi et. al [2] proposed a new a nonlinear, edge preserving and noise-reducing smoothing filter for images called Bilateral Filter. Bilateral filter [3] solves the limitation of Gaussian filter [4] by taking in account the difference in value with the neighborhood to preserve edges while smoothing. In bilateral filter, the influence of a pixel to another one should not only occupy a nearby location but also have a similar value. Though bilateral may not be the best noise reducing filter but it is good and simple. Also, it can be used for tone mapping, relighting and texture editing. However, the nonlinear operator is hard to compute since it is complex and spatially varying kernels. Besides, it causes staircase effect, gradient reversal, and artifact near edges. All the shortcomings are covered with the improved wih Guided image filter.

Guided image filter [5] is an edge preserving smoothing filter which output is locally a linear transform of the guidance image. It has good edge-preserving smoothing properties like bilateral filter but it solves the unwanted problems which occurs in bilateral filter. Guided filter has a O(N) time non-approximate algorithm, independent of the window radius and the intensity range. Also, it is easily implement and avoid staircase effect and artifacts. It is good to be applied in feathering, matting, single

image haze removal and joint up sampling. However, despite its advantage, guided filter also has its own limitation which is the exhibit halos near some edges when the image is being smoothing which is shown in Fig.5. Besides, it does not effectively reduce noise because its output values are unchanged within high-variance region.

Among methods in denoise using spatial domain, non-linear variational methods such ROF and TV-L1 total variational method [6, 7] were one of effective method to reduce noise but also keep edge-preserving. It bases on principle that signal detail is dense and smooth in variability. To obtain denoise image, it is an ill-pose problem with many solutions. So, the best solution is image with slowest variation or smoothness. All of properties above result to minimization problem with solving energy function with data term for assuming noise distribution with mean 0 and smoothness term about softness variability in details.

Approaching transform domain, image will transform into frequency domain to eliminate noise signals corresponding to "small" coefficients. Hard and soft thresholding will remove these values when they are less than specific thresholding. Wavelet shrinkage method [8] bases on thresholding of small wavelet coefficients. By eliminating theses values, the noise will be removed out of data. It takes pros than spatial domain method when keeping low contrast details. However, it produces many artifacts.

The current stat-of-the-art denoise methods is approach on taking advantages of spatial and transform domain. On spatial domain, these methods discover self-similarity in the image itself. In other words, they model patch space of an image and denoise by normalization similar patches. Besides, it will reduces noise signal in the patches by transforming frequency domain and thresholding small coefficients.

Dual-domain image denoise [9] is unmistakably simple method in implementing. Besides, it also has good results in PSNR comparing with different methods in same approach [10, 11]. However, because of using noise image for guided image, it also procedures artifacts as common errors of transform domain methods. Non-local dual

denoising [12] is a faster and better method more than Non-local dual denoising method. It avoids artifacts by applying NL-Bayes for building guided image. And it only uses one step to remove noise on spatial and frequency domain.

In this paper, we study about image denoising and review the pros and cons of spatial, transform and hybrid methods. In spatial domain, we study Bilateral filter, Guided image filter and TV-L1 total variational method. Next, in transform domain, we also introduce about Wavalet Shrinkage denoise. Last, we will study methods approaching spatial and transform domain for denoise such Dual Domain Image Denoise, Non-Local dual denoise.

The organization of this paper is as follows. In Section II, we introduce about image denoising and a synthesis of image filtering methods. Experiments results are discussed in Section III, followed by the conclusion and future work in the Section IV.

2. LITERATURE SURVEY

2.1. Spatial Domain

2.1.1. Bilateral Filter

In 1998, Carlo Tomasi and Roberto Manduchiis [2] proposed a new a nonlinear, edge preserving and noise-reducing smoothing filter for images called Bilateral Filter. Bilateral filter [3] solves the limitation of Gaussian filter [1-3] by taking in account the difference in value with the neighborhood to preserve edges while smoothing.

In bilateral filter, the influence of a pixel to another one should not only occupy a nearby location but also have a similar value which is defined by:

$$BF\left[I\right]_p \triangleq \frac{1}{w_p}\sum_{q\in S} G_{\sigma_S}\left(||p-q||\right) G_{\sigma_r}\left(|I_p - I_q|\right) I_q, \tag{1}$$

where G_{σ_S} is a spatial Gaussian weighting that decreases the influence of distant pixels, G_{σ_r} is a range Gaussian that decreases the influence of pixels q when their intensity value different from I_p, and W_p is normalization factor that ensures pixel weight sum to 1.0, defined by:

$$W_p = \sum_{q\in S} G_{\sigma_S}\left(||p-q||\right) G_{\sigma_r}\left(|I_p - I_q|\right) \tag{2}$$

The improvement in bilateral filter can clearly been seen when we compare the results in Fig. 1 which are got from applying bilateral filter and Gaussian filter [4, 1].

Bilateral filter is extremely easy to adapt. For color image, we can change the intensity difference to color difference in Eq.1 to get the desire output as below:

$$BF\left[I\right]_p \triangleq \frac{1}{w_p}\sum_{q\in S} G_{\sigma_S}\left(||p-q||\right) G_{\sigma_r}\left(|C_p - C_q|\right) C_q \tag{3}$$

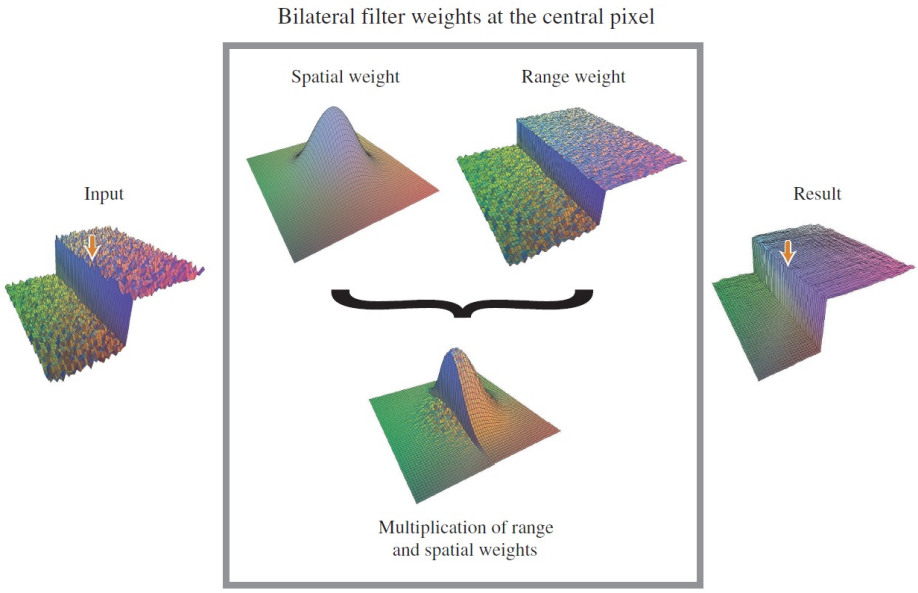

Figure 1: Bilateral filter for smoothing an input image [3]

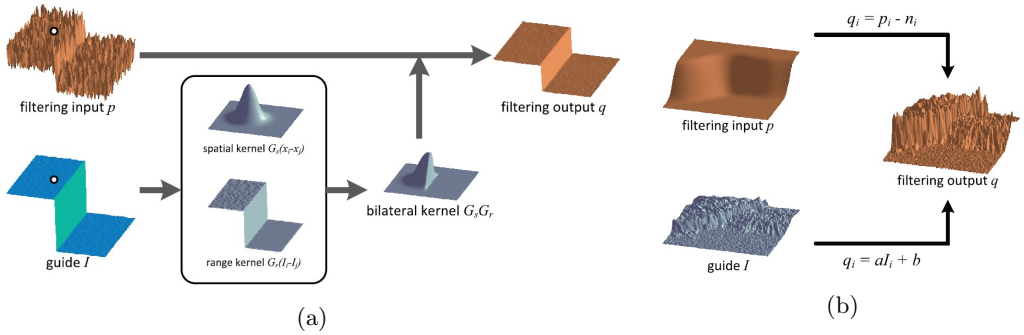

Figure 2: (a) Bilateral Filter Process and (b) Guided Filter Process

Though bilateral may not be the best noise reducing filter but it is good and simple. Also, it can be used for tone mapping, relighting and texture editing. However, the nonlinear operator is hard to compute since it is complex and spatially varying kernels. Besides, it causes staircase effect, gradient reversal, and artifact near edges.

2.1.2. Guided Image Filtering

Guided image filter [5] is an edge preserving smoothing filter, which output is locally a linear transform of the guidance image. It has good edge-preserving smoothing properties like bilateral filter but it solves the unwanted problems which occurs in

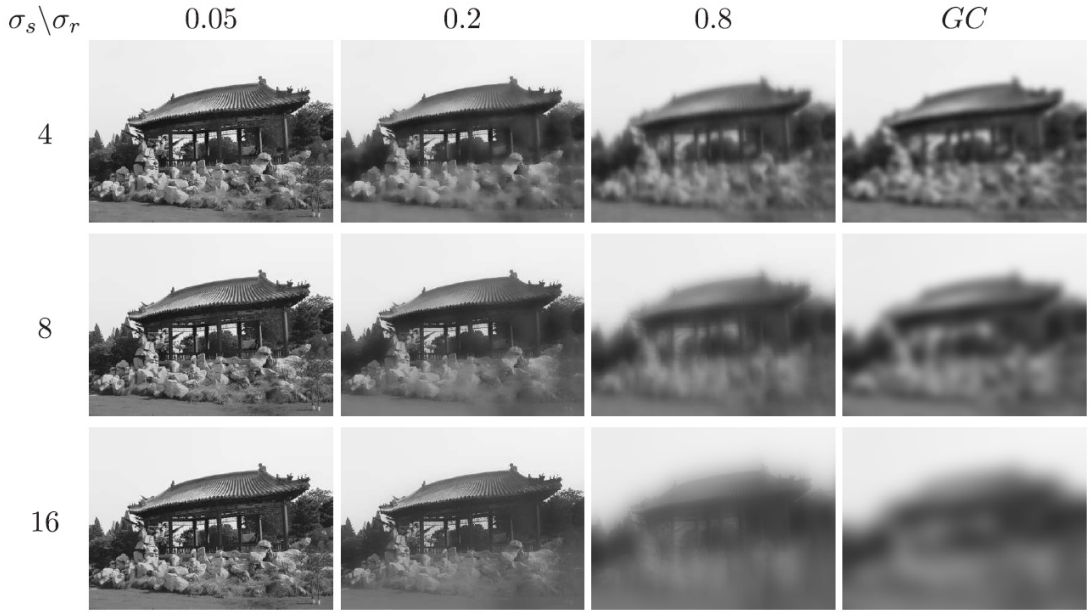

Figure 3: Comparison between Bilateral and Gauss Filter with increasing spatial and intensity parameter [3]

bilateral filter.

The guided filtering process involves a guidance image I, a filtering input image p and an output image q. Both I and p is given beforehand according to the application and they can be identical. Since we define that guided filter is a local linear model between the guidance image and the filtering output, we assume that q is a linear transform of I in a window ω_k centered at the pixel k and is defined by:

$$q_i = a_k I_i + b_k, \forall i \in \omega_k, where \begin{cases} a_k = \frac{\frac{1}{|\omega|}\sum_{i \in \omega_k} I_i p_i - \mu_k \bar{p}_k}{\sigma_k^2 + \epsilon} \\ b_k = \bar{p} - a_k \mu_k \end{cases} \tag{4}$$

In Eq. 4, μ_k and σ_k^2 are the mean and variance of I in ω_k, $|\omega|$ is the number of pixels in ω_k and $\bar{p}_k$ is the mean of p in ω_k.

We can also model the output q as the input p subtracting unwanted components

n as follows:

$$q_i = p_i - n_i \tag{5}$$

There are two cases in an input filter that should be consider which are "high variance" region and "flat patch". The idea of guided filter is that it determine "what is an edge that should be preserved"; hence, guided filter keep the high variance patch while the flat patch is smoothed which results in its good edge-preserving property. Not only guided filter can preserve edges, it can also preserve gradient and transfer structure. Guided image filter can be fast implemented with the following Alg. 1.

Algorithm 1: Guided Image Filtering

Input:
p: filtering input image.
I: guidance image.
r: radius.
ϵ: regularization.
Output:
q: filtering output image.

begin
- $mean_I = f_{mean}(I)$
- $mean_P = f_{mean}(P)$
- $var_I = corr_I - mean_I .* mean_I$
- $cov_{I_p} = corr_{I_p} - mean_I .* mean_p$
- $a = cov_{I_p} / (var_I + \epsilon)$
- $b = mean_p - a .* mean_I$
- $mean_a = f_{mean}(a)$
- $mean_b = f_{mean}(b)$
- $q = mean_a .* I + mean_b$

Note that f_{mean} is the mean filter [4], it can be replaced by Gaussian filter without having bad effect on performance of guided filter.

In the Fig. 4, we can clearly see that guided image can avoid staircase effect and artifact that bilateral filter has. The result got from guided image is much better than the one got from bilateral filter.

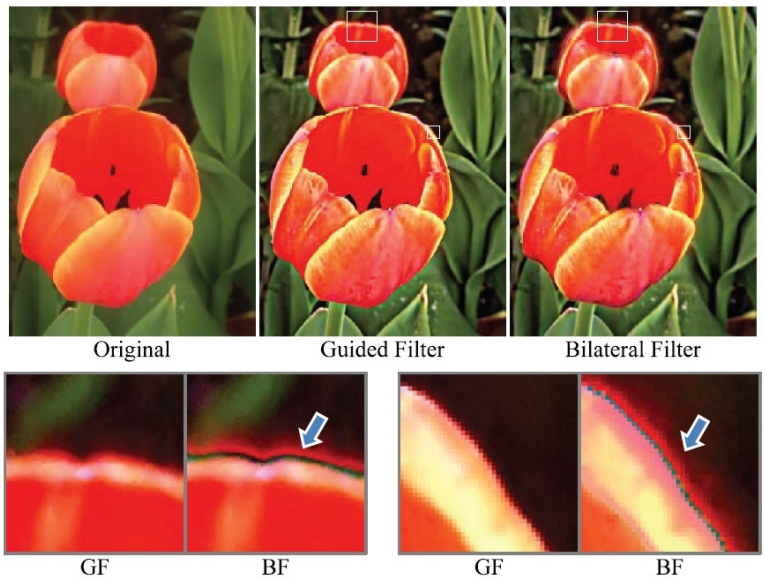

Figure 4: Detail enhancement comparing with Bilateral Filter with $r = 16, \epsilon = 0.1^2$ for Guided Filter , and $\sigma_s = 16, \sigma_r = 0.1$ for Bilateral Filter. [5]

To sum up, guided filter has a $O(N)$ time non-approximate algorithm, independent of the window radius and the intensity range. Also, it is easily implement and avoid staircase effect and artifacts. It is good to be applied in feathering, matting, single image haze removal and joint up sampling. However, despite its advantage, guided filter also has its own limitation which is the exhibit halos near some edges when the image is being smoothing which is shown in Fig. 5.

2.1.3. Non-linear variational methods with Total variational denoise

The total variational method is first mentioned in the inverse problem when proposing regularizing criteria. It is based on the principle that signal has smooth details. So, denoise becomes the minimization problem, which finds a image in set of all images with bounded variation. It is applied effectively in noise reduction with smoothing image but preserving the edges.[6]

The original image can be approximated by ideal and noise image as

$$f = u + n \tag{6}$$

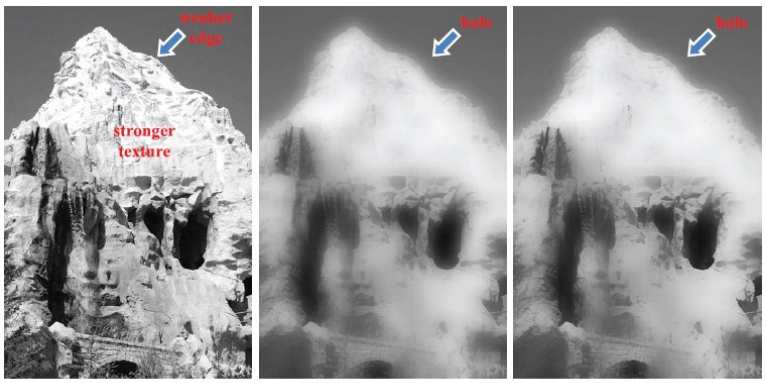

(a) input (b) guided filter (c) bilateral filter

Figure 5: The halo artifacts with $r = 16$, $\epsilon = 0.4^2$ for guided filter, $\sigma_s = 16$, $\sigma_r = 0.4$ for bilateral filter.[5]

where f is noisy image, u is ideal image and n is noise image which shows as Gaussian distribution with mean 0.

Observing that u has smooth in details, Rudin et. al [6] proposes the regularizing constraint for ensuing existing unique solution in an ill-posed problem for Eq.6 as

$$\min_{u \in BV(\Omega)} \int_{\Omega} |\nabla u\,(x)|\, dx \tag{7}$$

where first constraint assumes Gaussian Noisy with mean 0 as

$$\int_{\Omega} u\,(x)\, dx = \int_{\Omega} f\,(x)\, dx \tag{8}$$

and second constraint expresses noisy derivation σ as

$$\int_{\Omega} |u\,(x) - f\,(x)|^2\, dx = \sigma^2\, |\Omega| \tag{9}$$

In [7], Chambolle et. al changed Eq.7 into the following unconstrained minimization problem as

$$\min_{u \in BV(\Omega)} \int_{\Omega} |\nabla u|\, dx + \frac{\lambda}{2}\, ||u - f||\,|_2^2 dx \tag{10}$$

where first term is the smoothness term, second term is data term to evaluate the accuracy of data and λ is regularization constant.

Depend on normalization for the smoothness term, there are two model energy. First, ROF (Rudin, Osher and Fatemi) model uses L_1 normalization in the smoothness term as in Eq.10. Second, TV-L1 model uses L_2 normalization in data term as

$$\min_{u \in BV(\Omega)} \int_{\Omega} |\nabla u| \, dx + \lambda \, ||u\,(x) - f|\,| dx \tag{11}$$

TV-L1 and ROF models are the specific cases in general minimization energy problem[7, 13, 14] , which defined as

$$\min_{x} F\,(K_x) + G_x \tag{12}$$

where F and G are functions satisfying convex property, and K is linear operator. Clearly, data term and smoothness term in ROF and TV-L1 respectively express as

$$F\,(K_x) \triangleq \int |\nabla u| \tag{13}$$

$$G_{ROF} \triangleq \int \frac{\lambda}{2} \, ||x - f|\,|^2 \tag{14}$$

$$G_{TV-L1} \triangleq \int \lambda \, ||x - f|\,| \tag{15}$$

Applying the Legendre-Fenchel transformation for F with any $p \in X$, we obtain the dual formula F^* of F in Eq.12 as

$$F^*\,(p) = \sup_{x \in X} \langle p, x \rangle - F\,(X) \tag{16}$$

Similarly, applying the transformation for F^* where F and F^* are the convex

function, we obtain the formula below:

$$F = F^{**}(p) = \sup_{x \in X} \langle p, x \rangle - F^{*}(X) \tag{17}$$

Applying the above formula to F, we get the saddle formula as follows:

$$\min_{x} \max_{p} F(Kx, p) + G_x - F^{*}(p) \tag{18}$$

in which

$$F^{*}(p) = \sigma_P(p) = \begin{cases} 0 & p \in P \\ +\infty & p \notin P \end{cases} \tag{19}$$

where $P = \left\{ p : \forall_i \left\| p_i \right\| \leq 1 \right\}$

In primal-dual algorithm, we define proximity operator which is equivalent to implicit gradient descent step, as below

$$(I + \tau\delta F)^{-1}(x) = arg\min_{x} \frac{1}{2} \left\| y - x \right\|^2 + \tau F(y) \tag{20}$$

To implement Primal-Dual algorithm,F^* and G for ROF and TV-L1 are calculated as below

$$(I + \sigma\delta F^{*})^{-1}(p) = \frac{p}{max\left(\left\| p \right\|, 1 \right)} \tag{21}$$

$$(I + \tau\delta G_{ROF})^{-1}(x) = \frac{x + \lambda\tau f}{1 + \lambda\tau} \tag{22}$$

$$(I + \tau\delta G_{TV-L1})^{-1}(x) = \begin{cases} x - \lambda\sigma & x > f + \lambda\sigma \\ x + \lambda\sigma & x < f - \lambda\sigma \\ f & |x - f| \leq \lambda\sigma \end{cases} \tag{23}$$

Algorithm 2: Primal Dual Algorithm

Data:
+ Step size $\sigma > 0$, $\tau > 0$
+ $\sigma\tau L^2 < 1$, where $L = \|K\|$
+ $\theta = 1$
+ X: Input

begin
- $x_i = \mathrm{X}$;
- $p_i = \nabla x_i$;
- **while** *not convergence or not enough iteration* **do**
  - $p_i = (I + \sigma\delta F^*)^{-1}(p_i + \sigma K x_i)$; %Eq.21
  - %Eq.22 or 23
  - $\hat{x}_i = (I + \tau\delta G)^{-1}\left(x_i - \tau K^T p_i\right)$;
  - $x_i = \hat{x}_i + \theta(\hat{x}_i - x_i)$;

2.2. Frequency Domain using Wavelet Shrinkage Denoising

Wavelet shrinkage denoising [8] is considered a non-parametric method which attempts to remove noise and retain signal regardless of the frequency content of the signal. The basic idea behind this techniques is to use wavelets to transform the data into a different basis, where "large" coefficients correspond to the signal while "small" ones represent mostly noise. The wavelet coefficients are suitably modified and the denoised data is obtained by an inverse wavelet transform of the modified coefficients.

Let $\mathbf{Y}$, $\mathbf{X}$ and ϵ denote the observed data, the noiseless data and the error matrices respectively. The three main steps of denoising using the wavelet shrinkage technique are as follows:

- Calculate the wavelet coefficient matrix $\mathbf{w}$ by applying a wavelet transform $\mathbf{W}$ to the data:

$$\mathbf{w} = \mathbf{WY} = \mathbf{WX} + \mathbf{W}\epsilon \tag{24}$$

- Modify the detail coefficients to obtain the estimate $\mathbf{w}$ of the coefficients of $\mathbf{X}$:

$$\mathbf{w} \to \hat{\mathbf{w}} \tag{25}$$

- Inverse transform the modified coefficients to obtain the denoised estimate:

$$\hat{\mathbf{X}} = \mathbf{W}^{-1}\hat{\mathbf{w}} \tag{26}$$

Figure 6: (left) Noisy "Lena" image with $\epsilon = 20$ and (right) result output provided by Wavelet Shrinkage [8]

Observing Fig. 6, it notes that the noise is removed yet the detail of the image is not smooth compared to other spatial filters. However, the color contrast is not consistent as well as the computation complexity is high. Also, in some cases, wavelet shrinkage create noticeable artifact that can considerably degrade the image.

2.3. Integrated Spatial and Frequency Domain

2.3.1. Dual domain image denoising

Dual domain image denoising (DDID) [9] is an iterative denoising method which combines both spatial and transform domains. Since each domain has its advantages and shortcomings, this combination complements and solves the problems that effects on the result output.

Before DDID, there are several state-of-art approaches which combine both domain such as BM3D [15], shape-adaptive BM3D (SA-BM3D) [16] and BM3D with shape-adaptive principal component analysis (BM3D-SAPCA) [10]. They denoise based on block-matching which introduces visible artifacts in homogeneous regions, expressing as low-frequency noise. Also, they are sophisticated which pay for the high quality with implementation complexity [11].

DDID offers a simpler way to implement yet competes BM3D in quality. It combines two popular filters for two domains. For the spatial domain, the bilateral filter is used to preserve features like edges; however, it has difficulties preserving low contrast details. For the transform domain, short time Fourier transform [17] with wallet shrinkage [18, 19, 20, 8] is applied to preserve good detail though it suffers from ringing artifacts near steep edges.

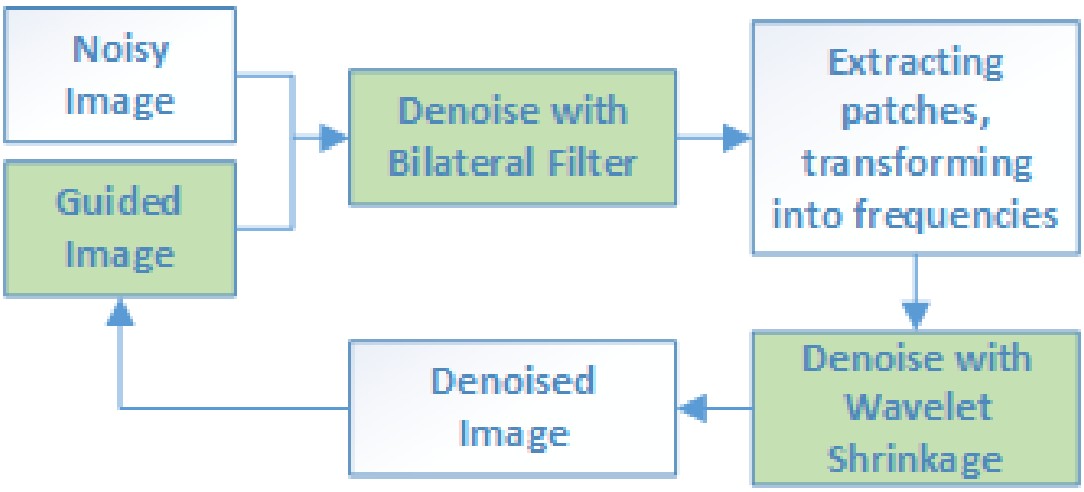

Figure 7: Dual Domain Image Denoising process

Given a noise-contaminated image $y = x + \eta$ with a stationary variance $\sigma^2 = Var[\eta]$, the goal of DIDD is to estimate the original image x. The image is separated into two layers which are denoised separately. The high-contrast layer is bilateral filtered and the low-contrast layer is denoised using wavelet shrinkage. Thus, the original

image can be approximated by the sum of two denoised layers as

$$\tilde{x} = \tilde{s} + \tilde{S}, \tag{27}$$

where $\tilde{s}$ and $\tilde{S}$ are the denoised high-contrast and low-contrast images.

In the first step, the denoised high-contrast values $\tilde{s}_p$ for a pixel p is computed using a joint bilateral filter [3]. The joint bilateral uses the guide image g to filter the noisy image y. The bilateral kernel is defined over a square neighborhood window $\mathscr{N}_p$ centered on every pixel p with window radius r. The parameter σ_s and γ_r shape the spatial and range kernels respectively. The two denoised image high-contrast images is obtain as following:

$$\tilde{g}_p = \frac{\sum_{q\in\mathscr{N}_p} k_{p,q} g_q}{\sum_{q\in\mathscr{N}_p} k_{p,q}} \tag{28}$$

$$\tilde{s}_p = \frac{\sum_{q\in\mathscr{N}_p} k_{p,q} y_q}{\sum_{q\in\mathscr{N}_p} k_{p,q}}, \tag{29}$$

where the bilateral kernel is

$$k_{p,q} = e^{-\frac{|p-q|^2}{2\sigma_s^2}} e^{-\frac{(g_p-g_q)^2}{\gamma_r\sigma_s^2}} \tag{30}$$

In the second step, for the wavelet shrinkage in the transform domain, the low contrast signals are extracted by subtracting the bilaterally filtered values $\tilde{g}_p$ and $\tilde{s}_p$ from g_p and y_p, followed by multiplication with the range kernel of Eq. 30. Then, the STFT is performed to transition these low-contrast signals to the frequency domain. The resulting coefficients $G_{p,f}$, and $S_{p,f}$, are presented for frequencies f in the frequency window $\mathscr{F}_p$ with the same size as $\mathscr{N}_p$.

$$G_{p,f} = \sum_{q\in\mathscr{N}_p} e^{-i2\pi(q-p).f/(2r+1)} k_{p,q} \left(g_q - \tilde{g}_p\right) \tag{31}$$

$$S_{p,f} = \sum_{q \in \mathcal{N}_p} e^{-i2\pi(q-p).f/(2r+1)} k_{p,q} \left(y_q - \tilde{s}_p\right) \tag{32}$$

Assuming that the bilateral kernel $k_{p,q}$ is noise-free, the variance $\sigma^2_{p,f}$ of the noisy Fourier coefficients is

$$\sigma^2_{p,f} = \sigma^2 \sum_{q \in \mathcal{N}_p} k^2_{p,q} \tag{33}$$

In the last step, shrinkage factors similar to the range kernel of the bilateral filter is used. For the wavelet shrinkage factor $K_{p,f}$, the signal needs keeping and the noise needs discarding:

$$K_{p,f} = e^{-\frac{\gamma_f \sigma^2_{p,f}}{|G_{p,f}|^2}} \tag{34}$$

Like the bilateral kernel $k_{p,q}$, the shrinkage factors $K_{p,f}$, are defined using the spectral guide $G_{p,f}$, and the wavelet shrinkage parameter γ_f plays a similar role as the bilateral range parameter γ_r. And the low-contrast value is yielded as following:

$$\tilde{S}_p = \frac{1}{|\mathscr{F}_p|} \sum_{f \in \mathscr{F}_p} K_{p,f} S_{p,f} \tag{35}$$

Dual domain image denoise can be fast implemented with the following Alg. 3.

2.3.2. Nonlocal dual denoising

DDID provides better quality of denoised output as well as a simpler way to implement denoising method in both spatial and transform domains than any other state-of-art algorithms sharing the same idea. However, its processing time is slow and it also causes strong frequency domain artifacts unexpectedly. A later approach named Nonlocal Dual Denoising (NLDD) [12] has overcome those drawbacks.

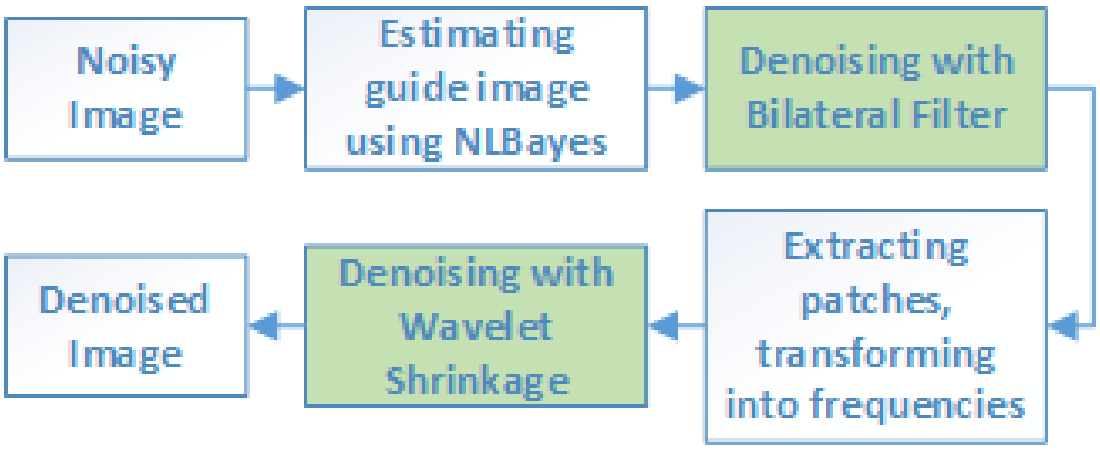

Figure 8: Non-local dual denoising process

The strong frequency domain artifacts are caused by the guide which is provided from the first two iterations of DDID algorithm. Since the DDID procedure is applied three times with different parameters, each time the result of the previous calculation is used as a guide. It notes that the image is denoised in the last iteration only and the other two are only used to obtain a suitable guide. Also, because of using the noisy image to be the guide in the first iteration and the kernel in Eq. 30 is computed from it, "parasite" information is reserved and transmitted in the following iterations. This yields a result that contains artifacts. Thus, NLDD chooses to use the guide image which is provided by NL-Bayes [11] because it has less artifacts than the one computed in the first two iteration of DDID.

Observing closely Fig. 9, it notes that the ringing artifacts in denoised image of DDID does not present in result of NLDD. Besides, the processing time of NLDD algorithm has reduced 3 times because of the reduction of iterations which occurs in DDID.

Figure 9: A detail of the artifacts produced by DDID and the corresponding result of NLDD. In this example $\sigma = 30$. [12]

Algorithm 3: Dual Domain Image Denoise

Data:
+ Bilateral range $\gamma_r = \{100, 8.7, 0.7\}$
+ Wavelet shrinkage $\gamma_f = \{4.0, 0.4, 0.8\}$
+ Window radius $r = 15$
+ Bilateral filter spatial $\sigma_s = 7$

```
function x = DDID(y, sigma2)
    x = step(y, y, sigma2, 15, 7, 100, 4.0);
    x = step(x, y, sigma2, 15, 7, 8.7, 0.4);
    x = step(y, y, sigma2, 15, 7, 0.7, 0.8);
end
function xt = step(x, y, sigma2, r, sigma_s, gamma_r, gamma_f)
    [dx dy] = meshgrid(-r:r);
    h = exp(-(dx.^2 + dy.^2) / (2 * sigma_s.^2));
    xp = padarray(x, [r r], 'symmetric');
    yp = padarray(y, [r r], 'symmetric');
    xt = zeros(size(x));
    parfor p = 1:numel(x), [i j] = ind2sub(size(x), p);
        %Spatial Domain: Bilateral Filter
        g = xp(i:i+2*r, j:j+2*r);
        y = yp(i:i+2*r, j:j+2*r);
        d = g - g(1+r, 1+r);
        k = exp(- d.^2 ./ (gamma_r * sigma2)) .* h;          %Eq.30
        gt = sum(sum(g .* k)) / sum(k(:));                   %Eq.28
        st = sum(sum(y .* k)) / sum(k(:));                   %Eq.29
        %Fourier Domain: Wavelet Shrinkage
        V = sigma2.* sum(k(:).^2) ;                          %Eq.33
        G = fft2(ifftshift((g - gt) .* k)) ;                 %Eq.31
        S = fft2(ifftshift((y - st) .* k)) ;                 %Eq.32
        K = exp(- gamma_f * V ./ (G .* conj(G))) ;           %Eq.34
        St = sum(sum(S .* K)) / numel(K) ;                   %Eq.35
        xt(p) = st + real(St) ;                              %Eq.27
    end
end
```

3. EXPERIMENTS AND DISCUSSIONS

3.1. Evaluation Measures

MSE (Mean-Square Error) is the average of the squares of the errors about difference between original image and restored image

$$MSE = \frac{1}{mn} \sum_{i=0}^{m-1} \sum_{j=0}^{n-1} [I(i,j) - K(i,j)]^2 \tag{36}$$

where I and K respectively are the original image and restored image with size $m \times n$.

RMSE (Root-mean-square error) is dervied from MSE as below

$$RMSE = \sqrt{MSE} \tag{37}$$

PSNR (Peak Signal to Noise Ratio) is a term used to calculate the ratio between the maximum energy value of a signal and the noise energy influences the accuracy of the information. Because there are many wide variation signals, the PSNR is usually represented by the dB unit. The bigger the PSNR is, the better the image is. The formula is used to calculate PSNR as below

$$PSNR = 10log_{10}\left(\frac{MAX_I^2}{MSE}\right) \tag{38}$$

where MAX_I is the maximum value of the pixel on the image.

3.2. Noise models

In this paper, we refer to the image noise problem caused by failure from gauss.The origin of Gauss noise in digital images is usually due to the sensor's image acquisition process affected by poor lighting, high temperature or signal transmission. Gauss noise is a addition, statistics noise with normal distribution. The probability density function

p of the Gaussian random variable z is given by the formula[4]:

$$p(z) = \frac{1}{\sqrt{2\pi\sigma}} e^{-(z-\mu)^2}/2\sigma^2 \tag{39}$$

where z represents the grey level, μ the mean value and σ the standard deviation.

Salt-and-pepper noise is a form of impulse noise caused by sharp and sudden disturbances in the image signal. Noise image will sparsely occurs white and black pixels. The probability density function p of the random variable z in salt-and-pepper noise is given by the formula[4]:

$$p(z) = \begin{cases} P_a & \text{with probability } a \\ P_b & \text{with probability } b \\ 0 & \text{otherwise} \end{cases} \tag{40}$$

where a and b are two positive numbers with $a + b < 1$, $[P_a, P_b]$ is pixel value domain.

3.3. Experiments

In paper, we implement benchmark for denoise methods introduced above. Bilateral method has code from OpenCV. Guided image filter implements from guide of author in [5]. In Guided image filter, we use guide images from bilateral filter and original filter. With TV-L1, we implements from [13]. Lastly, we use reports from [12] on homepage to take results of DDID and NLDD methods.

Table 1 shows comparison methods such bilateral filter, guided image filter using bilateral filter and original input for guided image:

Table 2 shows results of remain methods:

From Table 1 and 2, DDID and NLDD methods have results better than remain methods. They take advantages of spatial and transform domain in denoise. Besides, we also see that images with many details such as Trees image, Traffic image will take

Table 1: PSNR comparision among noise image, Bilateral filter, Guided image filter with guide image using Bilater and original image

	Noise	**Bilateral**	**Bilateral Guide**	**Original Guide**
Alley	11.6	20.51	20.94	24.44
Computer	11.96	20	19.99	24.36
Dice	11.67	22.44	24.51	36.84
Flowers	12.39	20.29	20.66	31.28
Girl	11.69	22.8	25.08	30.3
Traffic	11.78	19.83	19.74	23.35
Trees	11.82	18.3	17.63	19.41

Table 2: PSNR comparision among TV-L1, Dual-domain image denoise and non-local dual denoise method

	TVL1	**DDID**	**NLDD**
Alley	22.16	25.3	25.23
Computer	21.67	25.95	25.91
Dice	25.66	32.33	33.54
Flowers	21.84	28.81	29.46
Girl	26.47	32.11	32.94
Traffic	21.41	24.63	24.77
Trees	18.25	20.25	20.46

lower results for all methods as Fig.10.

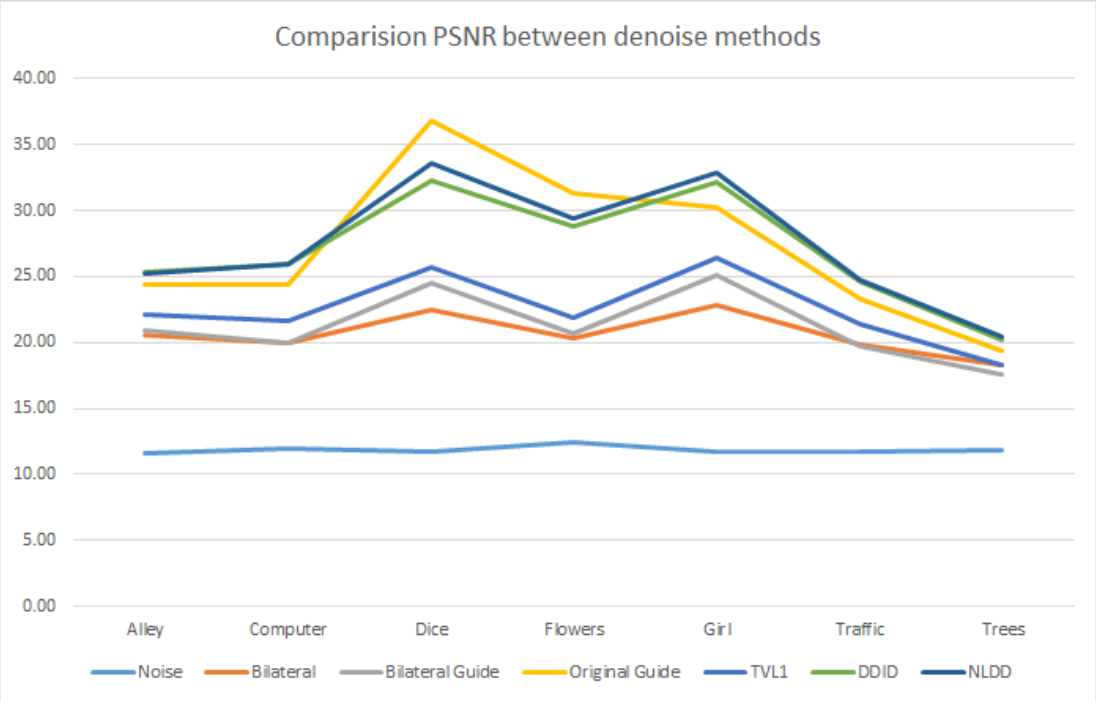

Figure 10: Comparision PSNR between denoise methods

(a) Original Image

(b) Gauss noisy images with $\sigma = 80$

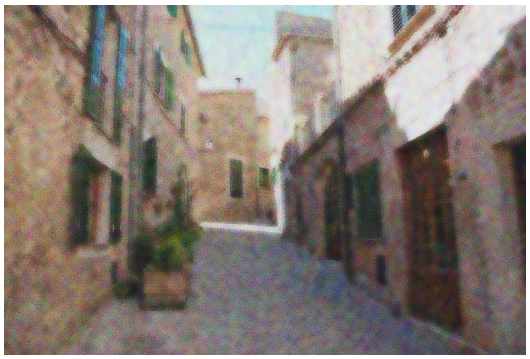

(c) Bilateral with PSNR = 20.508

(d) Bilateral Guided Image Filter with PSNR = 20.94

Figure 11: Alley image with noise

(a) Original Guided Image Filter with PSNR = 24.44

(b) TVL1 with PSNR = 22.16

(c) DDID with PSNR = 25.30

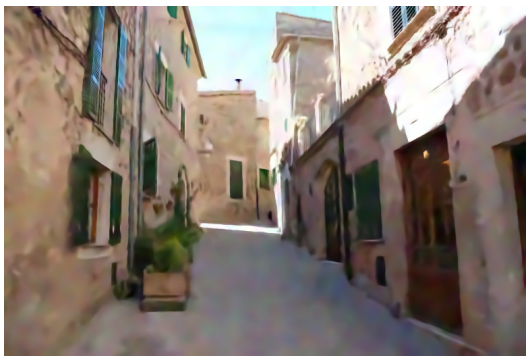

(d) NLDD with PSNR = 25.23

Figure 12: Alley image denoise

4. CONCLUSIONS

To sum up, paper makes a survey for denoise methods. Bilateral filter, guided image filter and total variational methods process by spatial domain. In which, total variational method has good result more than remain methods. Besides, the results also shows NLDD, DDID are effective methods in denoise with not only hybrid approach but also spatial methods. From the survey, denoise also has many challenges when denoising on images too small details.

REFERENCES

[1] M.C. Motwani et al. "Survey of image denoising techniques". In: *Proceedings of GSPx*. 2004, pp. 27–30.

[2] C. Tomasi and R. Manduchi. "Bilateral filtering for gray and color images". In: *Sixth International Conference on Computer Vision (IEEE Cat. No.98CH36271)* (1998), pp. 839–846. ISSN: 1873622X. DOI: 10.1109/ICCV.1998.710815.

[3] Sylvain Paris et al. "Bilateral Filtering: Theory and Applications". In: *Foundations and Trends® in Computer Graphics and Vision* 4.1 (2008), pp. 1–75. ISSN: 1572-2740. DOI: 10.1561/0600000020.

[4] Rafael C Gonzalez and Richard E Woods. *Digital Image Processing (3rd Edition)*. Upper Saddle River, NJ, USA: Prentice-Hall, Inc., 2006. ISBN: 013168728X.

[5] Kaiming He, Jian Sun, and Xiaoou Tang. "Guided image filtering". In: *IEEE Transactions on Pattern Analysis and Machine Intelligence* 35.6 (2013), pp. 1397–1409. ISSN: 01628828. DOI: 10.1109/TPAMI.2012.213.

[6] Leonid I Rudin, Stanley Osher, and Emad Fatemi. "Nonlinear total variation based noise removal algorithms". In: *Phys. D* 60.1-4 (1992), pp. 259–268. ISSN: 0167-2789. DOI: http://dx.doi.org/10.1016/0167-2789(92)90242-F.

[7] Antonin Chambolle et al. "An Introduction to Total Variation for Image Analysis". In: *Theoretical foundations and numerical methods for sparse recovery* 9 (2010), pp. 263–340. DOI: 10.1515/9783110226157.263.

[8] Imola K Fodor and Chandrika Kamath. "Denoising through wavelet shrinkage: an empirical study". In: *Journal of Electronic Imaging* 12.1 (2003), pp. 151–160.

[9] Claude Knaus and Matthias Zwicker. "Dual-domain image denoising". In: *IEEE International Conference on Image Processing, ICIP 2013 - Proceedings* 4 (2013), pp. 440–444. ISSN: 1522-4880. DOI: 10.1109/ICIP.2013.6738091.

[10] Kostadin Dabov et al. "BM3D image denoising with shape-adaptive principal component analysis". In: *Proc. Workshop on Signal Processing with Adaptive Sparse Structured Representations* (2009), p. 6. ISSN: 0277786X. DOI: 10.1117/12.643267.

[11] Marc Lebrun. "An Analysis and Implementation of the BM3D Image Denoising Method". In: *Image Processing On Line* 2.May (2012), pp. 175–213. ISSN: 2105-1232. DOI: 10.5201/ipol.2012.l-bm3d.

[12] N. Pierazzo et al. "Non-local dual image denoising". In: *2014 IEEE International Conference on Image Processing, ICIP 2014*. 2014, pp. 813–817. ISBN: 9781479957514. DOI: 10.1109/ICIP.2014.7025163.

[13] Alexander Mordvintsev. *ROF and TV-L1 denoising with Primal-Dual algorithm*. 2013. URL: https://github.com/znah/notebooks/blob/master/TV%5C_denoise.ipynb.

[14] Joan Duran, Bartomeu Coll, and Catalina Sbert. "Chambolle's Projection Algorithm for Total Variation Denoising". In: *Image Processing On Line* 2013 (2013), pp. 311–331. ISSN: 2105-1232. DOI: 10.5201/ipol.2013.61.

[15] Kostadin Dabov et al. "Image restoration by sparse 3D transform-domain collaborative filtering". In: *Proceedings of SPIE-IS&T, Image Processing: Algorithms and Systems VI, San Jose, California, USA, 28 January 2008* 6812.213462 (2008), p. 12.

[16] Kostadin Dabov et al. “a Nonlocal and Shape-Adaptive Transform-Domain Collaborative Filtering”. In: *Proc. Int. Workshop on Local and Non-Local Approx. in Image Process.* x (2008), p. 9.

[17] J Allen. “Short term spectral analysis, synthesis, and modification by discrete Fourier transform”. In: *Acoustics, Speech and Signal Processing, IEEE Transactions on* 25.3 (1977), pp. 235–238. ISSN: 0096-3518. DOI: 10.1109/TASSP.1977.1162950.

[18] David L. Donoho et al. “Wavelet Shrinkage: Asymptopia?” In: *Journal of the Royal Statistical Society. Series B (Methodological)* 57.2 (1995), pp. 301–369. ISSN: 0035-9246. DOI: 10.2307/2345967.

[19] Xuli Zong. “De-noising and contrast enhancement via wavelet shrinkage and nonlinear adaptive gain”. In: *Proceedings of SPIE* 2762 (1996), pp. 566–574. ISSN: 0277786X. DOI: 10.1117/12.236028.

[20] Carl Taswell. “The What How, and Why of Wavelet Shrinkage Denoising”. In: *Computing in Science and Engineering* 2.3 (2000), pp. 12–19. ISSN: 15219615. DOI: 10.1109/5992.841791.

이미지 노이즈 제거에 대한 설문조사

응우옌 반 타이

전남대학교 대학원 인공 지능 융합학과

(지도교수: 김용비)

(국문초록)

노이즈 제거는 디지털 이미지 처리 시스템의 전처리 단계입니다. 또한 전형적인 이미지 처리 문제입니다. 새로운 접근 방식으로 문제를 해결하기 위해 많은 작업이 제안되었습니다. 공간 기반 또는 변환 기반의 두 가지 주요 범주로 나눌 수 있습니다. 일부 잡음 제거 방법은 공간 및 변환 영역 모두에 적용됩니다.

이 문서의 목표는 잡음 제거 방법을 검토하고 이를 다양한 범주로 분류하고 새로운 경향을 식별하는 데 중점을 둡니다. 또한 설문 조사 방법의 장단점을 비교하기 위해 실험을 수행합니다.

ACKNOWLEDGEMENT

Foremost, I would like to sincerely thank Professor ... for guiding me with useful comments, suggestions, and support during my research and writing this thesis. I will also be grateful to him for enlightening me on research and his valuable advice on my life's future goal. Since he always provides willing supports for our lab with the best research conditions, my study has been comfortably and favorably completed.

I would also like to thank all current and former members of the ... Lab, ..., to support all the consumable items and good facilities to go through the whole process projects with the best conditions.

Finally, I would like to thank my parents, family, relationships, and friends in Korea and ... for their love and attention during my time away from home. Without them, this would not be possible.